

Improved Oil Slick Identification Using CMOD5 Model for Wind Speed Evaluation on SAR Images

Horiya KHENOUCHE and Youcef SMARA, Algeria

Key words: SAR images, oil spill, lookalikes, wind, CMOD4, CMOD5.

SUMMARY

The capacity of synthetic aperture radar to observe the sea surface, its potentiality for evaluating the wind vector, for the interpretation of atmospheric and oceanic phenomena make the radar SAR a useful tool in the control and surveillance of oil spill pollution on sea surfaces.

The wind is the most important phenomena that affect the appearance of the sea surface on radar images. It can cause or modify several atmospheric and oceanic phenomena. In particular, the wind can change the shape of oil slicks, or causes lookalikes.

The visibility of oil spills and their identification from radar images are particularly dependent on wind speed. For this reason, we've included the wind speed in order to improve the identification of oil slicks process.

Wind speed is calculated using the CMOD5 model. This is a model for wind vector evaluation, initially developed for radar scatterometers, it gives the backscattering coefficient according to wind speed, wind direction and incidence angle. The model, however, can be applied to the radar SAR images.

The inversion of the CMOD5 model allows the calculation of wind speed from a SAR image but with an interactive pre-estimate wind direction on the image. This interactive inspection is based mainly on the interpretation of atmospheric phenomena.

In this paper we describe the performance of CMOD5 based on CMOD4 with approximation of coefficients, we have used CMOD5 to calculate the wind speed and to compare it with wind speed calculated from CMOD4 for oil spills identification using SAR images on Algerian coasts acquired by ERS2 satellite.

RESUME

La capacité de radar à synthèse d'ouverture à observer la surface de la mer , sa potentialité pour évaluer le vecteur vent, pour l'interprétation des phénomènes atmosphériques et océaniques fait du radar SAR un outil utile dans le contrôle et la surveillance de la pollution en cas de déversement d'hydrocarbures sur la surface des mers .

Le vent est un des phénomènes les plus importants qui affectent l'apparence de la surface de la mer sur les images radar. Il peut provoquer ou modifier plusieurs phénomènes atmosphériques et océaniques. En particulier, le vent peut changer la forme de nappes de pétrole, ou provoque des sosies de nappes .

La visibilité des déversements d'hydrocarbures et leur identification à partir d'images radar sont particulièrement tributaires de la vitesse du vent . Pour cette raison, nous avons inclus la vitesse du vent afin d'améliorer l'identification des processus de nappes de pétrole.

La vitesse du vent est calculée en utilisant le modèle CMOD5. Il s'agit d'un modèle d'évaluation vecteur vent, initialement développé pour des diffusiomètres radar. Il donne le coefficient de rétrodiffusion en fonction de la vitesse du vent, direction du vent et l'angle d'incidence. Le modèle, cependant, peut être appliqué aux images radar SAR .

L'inversion du modèle CMOD5 permet le calcul de la vitesse du vent à partir d'une image SAR mais avec une pré- estimation direction du vent interactif sur l'image . Cette inspection interactive est basée principalement sur l'interprétation des phénomènes atmosphériques .

Dans cet article, nous décrivons les performances de CMOD5 basé sur CMOD4 avec rapprochement des coefficients , nous avons utilisé CMOD5 pour calculer la vitesse du vent et pour la comparer avec la vitesse du vent calculée à partir CMOD4 pour l'identification des déversements de pétrole en utilisant des images SAR sur les côtes algériennes acquises par satellite radar ERS-2.

Mots Clé: Images radar SAR, nappes d'hydrocarbures, vitesse du vent, CMOD4, CMOD5.

Improved Oil Slick Identification Using CMOD5 Model for Wind Speed Evaluation on SAR Images

Horiya KHENOUCHE and Youcef SMARA, Algeria

1. INTRODUCTION

The Mediterranean Sea is a well-frequented sea route allowing access to southern Europe, North Africa, the Middle East and the Black Sea. The result of this extensive marine traffic is a high risk of oil pollution, a problem that Earth Observation may be in a position to solve (Fontanel, 1973). Among other applications, imaging radar SAR is expected to play a major role in the detection of oil spills present on the coastal and marine areas. Several projects have been identified for the demonstration of the utility of satellite SAR radar images for the early detection of oil spill at sea or in coastal areas (Bern, 1993).

The influence of atmospheric conditions in the detection of oil spills is major: When the sea is slight or moderate, mitigating the bustle of the sea surface caused by the presence of oil spill, resulting in the decrease the value of the radar backscatter coefficient (Hamre, 1996). This is shown in the radar images, by a dark surface indicating the presence of the oil spill. When the wind speed is low, the sea surface is calm causing several natural phenomena with radar signatures similar to those of oil slicks. When the sea is very rough, the density and viscosity of the oil spill and enhance the buoyancy of the oil spill becomes uncertain. If the oil spill is immersed it becomes not detectable by the radar.

However, the characteristic of "lookalikes slicks" SAR imaging radar is that it can be interpreted as an oil slick when in reality it is the result of other oceanographic phenomena and /or weather (meteorologic).

Many natural phenomena can have the same radar that oil slicks signature. Physical and geometrical parameters of the water alone are not always sufficient to provide the information necessary for identification. Additional data such as wind speed calculated from radar images have demonstrated their effectiveness (Espedal, 1999) .

We have also implemented an evaluation process wind vector that plays an important role in the identification of oil spills. Indeed, the wind is regarded as the parameter principal that modifies the surface of the seas and oceans. To identify the oil slicks on radar images, the process used must be able to analyze radiometric characteristics and geometric suspicious oil spill, and the conditions that surround (Del Frate, 2000). The high number and complexity of these features may generate long and complex process for the development of identification rules. The neural approach is a flexible and effective tool for automatic processing of data which the statistical behavior is complex. We opted for a neural approach based on the analysis of physical and geometrical characteristics of the suspect oil spill and the wind speed. The features of the object are then calculated and presented to the input of a multilayer neural network trained by the backpropagation algorithm (Bouchaib, 2004).

The purpose of this study is: improving oil slicks identification by introducing wind speed as a new input of the neural network. For this, we have developed a method for estimating the wind direction which is based on the interpretation of atmospheric phenomena present on SAR PRI images. Then, we calculated the wind speed using the CMOD5 model. The results and validation of the method for estimating the wind vector applied on SAR PRI images of Algerian coasts are presented.

2. METHODOLOGY

To differentiate oil slicks from lookalikes on radar images, we have developed a process of identification based on a neural network using the physical and geometric parameters of suspicious object. But these are not always sufficient to recognize the nature of the oil spill. Additional data, such as wind speed is needed to improve the performance of this process. We developed a neural network which takes into account, in addition to the physical and geometrical parameters, the wind speed in the identification process. We calculated the wind speed using CMOD4 and CMOD5 model, empirical models that determine the coefficient radar backscatter depending on the speed and direction of wind vector and the incidence angle of the satellite. We have reversed the models, which we used to calculate the wind speed but with a pre- estimate of the direction. To do this, we conducted a comprehensive study that visually estimates the direction of the wind vector from radar images. This estimation is mainly based on the inspection and interpretation of atmospheric and oceanic phenomena.

Several authors have focused on developing methods for the detection and identification of signatures of oil spills from SAR images (Bjerde, 1993) (Solberg, 1999) (Kanaa, 2003) (Mercier, 2003) according to these authors, the process can be summarized in three phases (Konstantinos, 2008):

- 1-Screening and detection of dark spots present in SAR images.
- 2-Characterization of signatures detected, and the surrounding environment.
- 3-Classification of the extracted signatures.

The general process of this methodology is given in Figure 1:

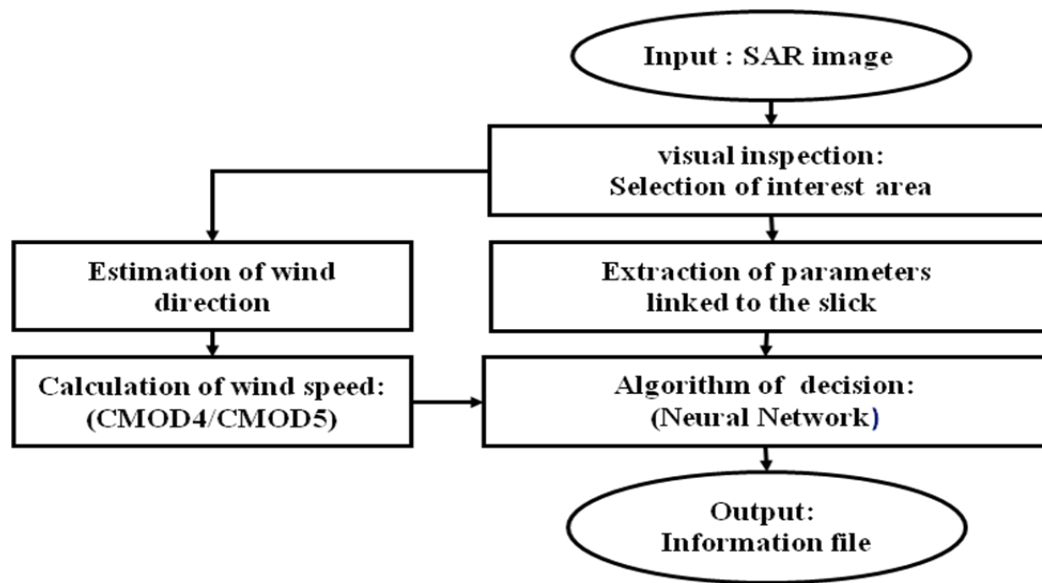


Figure 1. Block-diagram of the identification method

The identification method is presented in the following procedures:

- 1) Selection of interest region (containing suspicious object).
- 2) Estimation of wind direction.
- 3) Calculation of wind speed.
- 4) Calculation of physical and geometrical parameters characterizing the object.
- 5) Decision on the nature of the suspected object (oil spill/ not oil spill).

2.1 Selection of Interest Areas

For our study, we use the areas selected from two SAR PRI images taken on the Algerian coast (Figure 2). The first image shows the coast of El -Kala (east of Algeria) acquired on 22/09/2002. The second image acquired on 22/05/2000 represents the coast of Oran (West of Algeria).

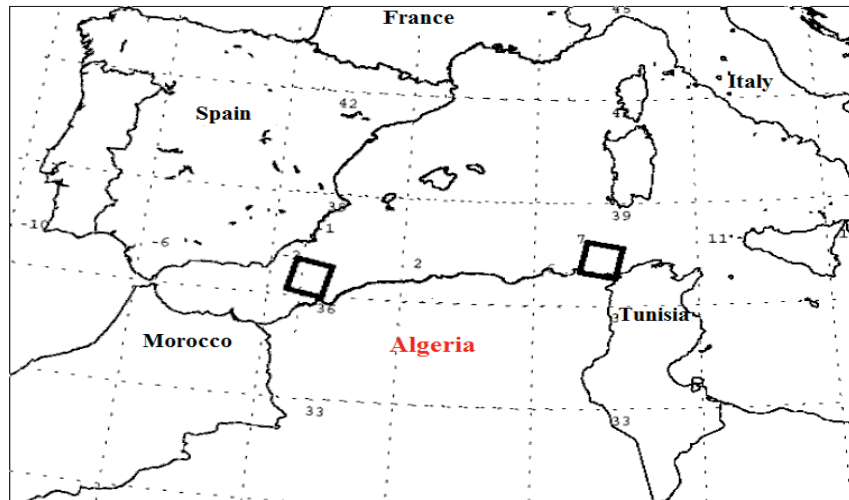


Figure 2: Location of El -Kala (east of Algeria) and Arzew (West of Algeria) images

The first step consists of a selection of the interest area with the suspect object . The procedure then allows the detection of the object with the largest dark surface in the area.

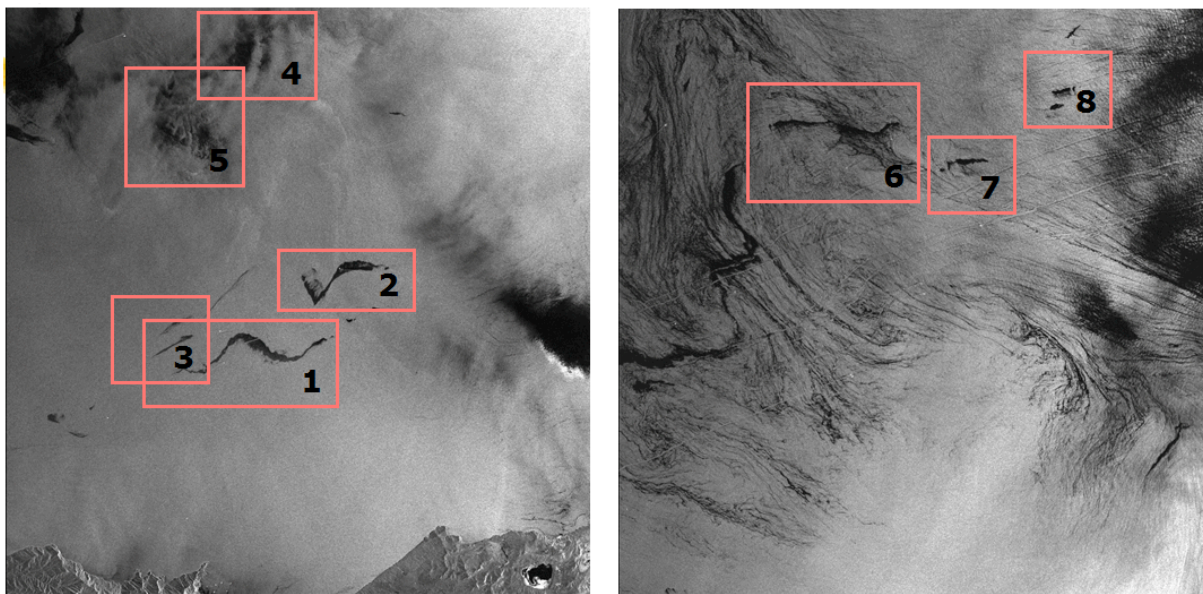


Figure 3: Selection of interest areas on the two images of El -Kala and Arzew (Algeria)

We have selected eight interest areas, five zones on the image of Elkala and three zones on the image of Arzew.

Images below show the result of edge detection by the method of ant:

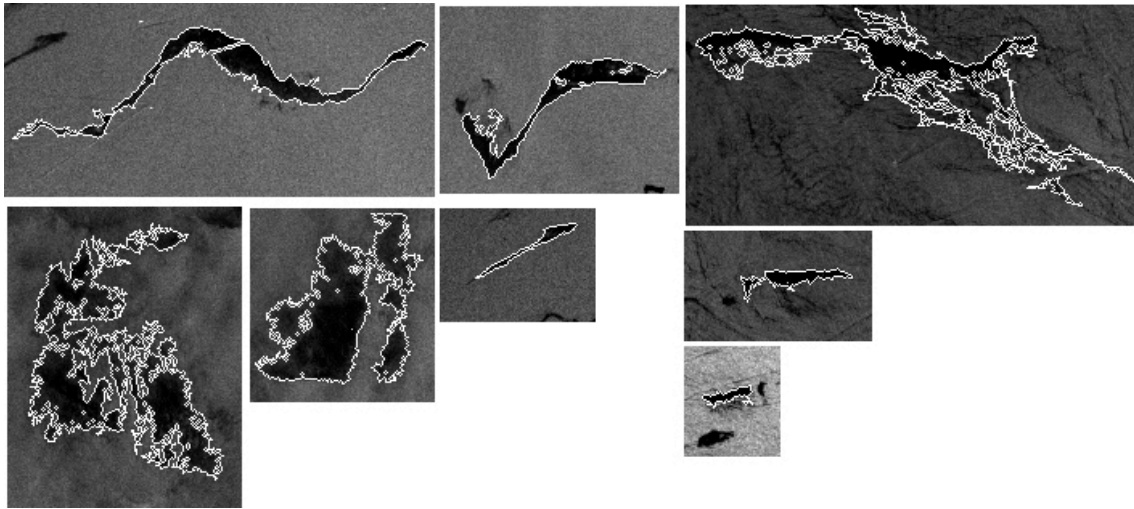


Figure 4: Result of edge detection image of El -Kala and image of Arzew.

2.2 Estimation of Wind Direction

There are many natural and atmospheric phenomena that allow to estimate the wind direction with interactive estimation. This interactive inspection is mainly based on the interpretation of atmospheric and oceanic phenomena

The wind is the most atmospheric phenomenon that change the sea surfaces to modulate the radar backscatter coefficient (Figure 5).

The maximum wind-induced phenomena are then collected to estimate the wind direction (eg: the presence of atmospheric gravity waves that appear downwind of mountainous coastal zones, perpendicular to the wind direction) (Mastin, 1985) .

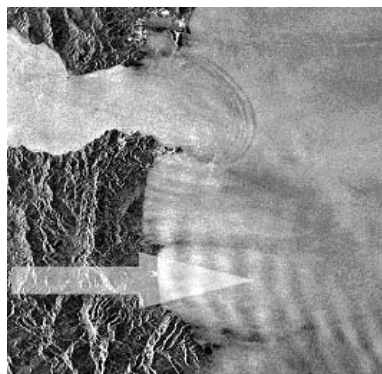


Figure 5: Atmospheric gravity waves generated by a west wind through a mountainous coastal .

2.3 Calculation of Wind Speed

We used two empirical models that determine the radar coefficient backscatter depending on the wind vector's speed and direction and the incidence angle of the satellite, CMOD4 and CMOD5 model.

2.3.1. CMOD4 model

The CMOD4 (Scatterometer transfer function for the ERS scatterometer C- band) is an empirical estimation model of the wind vector developed for radar ERS- 1/2 (Lecomte, 1993) scatterometer .It gives the backscatter coefficient σ^0 based wind speed V , of the wind direction relative to the view angle of φ and the angle of incidence θ of the radar according to the following formula (Stoffelen, 1997):

$$\sigma^0 = b_0 (1 + b_1 \cdot \cos\varphi + b_3 \cdot \text{Tanh}(b_2) \cdot \cos(2\varphi))^{1,6}$$

The coefficients b_0, b_1, b_2 and b_3 are coefficients dependent on the incidence angle and of the local wind speed. They are given by the following equations:

$$\left\{ \begin{array}{l} b_0 = b_r \times 10^{\alpha + \gamma \cdot f(V + \beta)} \\ b_1 = (c_{10} + c_{11} \cdot V) + \varepsilon(c_{12} + c_{13} \cdot V) \\ b_2 = c_{14} + c_{15} \cdot (1 + p_1) \cdot V \\ b_3 = 0.42 \cdot (1 + c_{16} (c_{17} + p_1)(c_{18} + V)) \end{array} \right.$$

Where $\varepsilon = \tanh(2.5(p_1 + 0.35)) - (0.61(p_1 + 0.35))$

and P_1, P_2 polynomial defined as follows :

$$P_1 = \frac{\theta - 40}{25} \quad P_2 = \frac{3P_1^2 - 1}{2}$$

$$\text{and } f(x) = \begin{cases} -10 & \text{if } x \leq 0 \\ \log_{10}(x) & \text{if } 0 < x \leq 5 \\ 0.31\sqrt{x} & \text{if } x > 5 \end{cases}$$

$$\begin{cases} \alpha = c_1 + c_2.P_1 + c_3.P_2 \\ \gamma = c_4 + c_5.P_1 + c_6.P_2 \\ \beta = c_7 + c_8.P_1 + c_9.P_2 \end{cases}$$

$c_1 \dots c_{18}$ and br are constants calculated from the characteristic parameters CMOD4 model. They are given in (Lecomte, 1993).

2.3.2. CMOD5 model

The CMOD5 is a new C-band geophysical model function that improve the calculation of wind speed.

The form of the CMOD5 model is (Hersbach, 2005):

$$\sigma^0 = B0(1 + B1.\cos \varphi + B2.\cos 2\varphi)^{1.6}$$

where B_0 , B_1 and B_2 are functions of wind speed v and incidence angle θ , or alternatively,

$$x = (\theta - 40)/25.$$

The B_0 term is defined as:

$$B_0 = 10^{a_0+a_2v} f(a_2v, s_0)^\gamma$$

Where

$$f(s, s_0) = \begin{cases} \left(\frac{s}{s_0}\right)^\alpha g(s_0), s < s_0 \\ g(s), s \geq s_0 \end{cases}$$

Here

$$g(s) = 1/(1 + \exp(-s))$$

$$\alpha = s_0(1 - g(s_0))$$

The functions a_0 , a_1 , a_2 , γ and s_0 depend on incidence angle only:

$$a_0 = c_1 + c_2x + c_3x^2 + c_4x^3$$

$$a_1 = c_5 + c_6x$$

$$a_2 = c_7 + c_8x$$

$$\gamma = c_9 + c_{10}x + c_{11}x^2$$

$$s_0 = c_{12} + c_{13}x$$

The B1 term is modeled as follows:

$$B1 = \frac{c_{14}(1+x) - c_{15}v(0.5+x - \tanh[4a_3])}{1 + \exp(0.34(v - c_{18}))}$$

Where

$$a_3 = x + c_{16} + c_{17}v$$

The B2 term was chosen as:

$$B2 = (-d_1 + d_2v_2) \exp(-v_2)$$

Here v_2 is given by:

$$v_2 = \begin{cases} a + b(y-1)^n, & y < y_0 \\ y, & y \geq y_0 \end{cases}$$

$$y = \frac{v + v_0}{v_0}$$

Where

$$y_0 = c_{19}$$

$$n = c_{20}$$

$$a = y_0 - (y_0 - 1)/n$$

$$b = 1/[n(y_0 - 1)^{n-1}]$$

The quantities v_0 , d_1 and d_2 are functions of incidence angle only:

$$v_0 = c_{21} + c_{22}x + c_{23}x^2$$

$$d_1 = c_{24} + c_{25}x + c_{26}x^2$$

$$d_2 = c_{27} + c_{28}x$$

2.4 Calculation of Physical and Geometrical Parameters Characterizing the Object

The features extracted from the dark object are input to the neural network that estimates its probability of being an oil slick. These features consider the geometry of the dark object in term of its extension and of its shape, as well as the physical behavior in terms of the characteristics of the backscattering intensity of the pixels belonging to the object, to the background, and to the area around the border (Del Frate, 2000).

After defining suspicious objects (the eight zones selected on the two used images), We have calculated the most used parameters characterizing it, features extracted are:4 geometric parameters and 7 statistics parameters.

Geometric parameters:

- Oil spill surface (A) :Area of the object.
- Perimeter (P) : length of the border of the object.
- Complexity (C) :this feature will generally take a small numerical value for regions with simple geometry and larger values for complex geometrical regions.
- Dissemination (S) :Spreading

Statistic parameters:

- Object standard deviation (OSd) :Standard deviation of the intensity values of the pixels belonging to the oil spill candidate.
- Background standard deviation (BSd) :Standard deviation of the intensity values of the pixels belonging to the region of interest, surrounding the object.
- Maximum contrast (ConMax) : Difference between the background mean value and the lowest value inside the object.
- Mean contrast (ConMe) :Difference between the background mean value and the object mean value.
- Maximum gradient (GMax) :Maximum value of border gradient.
- Mean gradient (GMe) :Mean border gradient.
- Gradient Standard deviation (GSd) : Standard deviation of the border gradient values.

Parameters calculated for each zone and wind speed calculated from the two models CMOD4 and CMOD5 are presented in the following table :

Parameters	Zone 1	Zone 2	Zone 3	Zone 4	Zone 5	Zone 6	Zone 7	Zone 8
A (Km²)	17.48	26.61	3.03	54.64	76.8	62.64	2.52	1,95
P(Km)	43.30	76.70	13.70	110.7	250.20	190.25	11.25	9,25
C	5.4	4.01	2.22	5.22	8.05	6.52	2.5	2.2
S	5,20	7,64	1,22	28,52	30,01	29,11	2,1	2,1
OsD	2.61	2.59	1.64	2.35	1.89	2.12	1.50	0.22
BSd	0.91	0.84	0.71	1.41	1.38	1.25	0.62	0.31
ConMax	15.38	13.85	8.59	13.58	10.33	12.55	8.62	7.54
ConMe	8.64	6.46	5.44	6.4	5.48	5.94	5.21	4.34
GMax	15.16	9.05	6.94	7.01	6.59	6.7	5.83	6.47
GMe	7.2	2.99	3.18	3.2	2.64	3.0	2,54	3.22
GSd	1.42	1.31	1.39	1.53	0.94	1.23	1.28	1.21
V(CMOD4)	4.1	4.1	3.9	2.4	2.1	1.9	2.1	2.4
V(CMOD5)	5.4	5.4	5.2	3.7	3.4	3.2	3.4	3.7

Table 1:parameters linked to the object selected on used SAR images

2.5 Decision on the Nature of the Suspected Object (oil spill/ not oil spill)

After calculating the different parameters that are inputs of the neural network, we performed the identification of the eight zones using both networks prepared either the 11 entries (without the wind speed input) and one with 12 inputs (integrating wind speed input calculating by two models CMOD4 and CMOD5). When the probability exceeds 0.7, the suspect object is considered as slick and when this probability is less than 0.3, the oil spill is considered a lookalike. The identification of eight areas suspected is given in table 2:

ZONE	Without wind speed	CMOD4	CMOD5
1	41%	89%	99%
2	85%	92%	99%
3	92%	95%	99%
4	1%	2%	0.004%
5	7%	6%	0.5%
6	8%	3%	4%
7	72%	81%	99%
8	92%	96%	99%

Table 2: Comparison between the results of identification

DISCUSSIONS AND CONCLUSION

The objective of this work is to work out an operational tool of detection and identification of oil spills starting from images radar based on the neural networks. The process of identification is established on the basis of the geometrical characterization of the object to identify and the estimate the wind speed. From the results obtained, we can draw the following conclusions: The three processes of identification developed, including or not the parameter wind speed in their bases of training, gave encouraging rates of recognition. We noted that CMOD4 and CMOD5 processes including the wind speed provided more powerful results. Indeed, the effect of the parameter wind on the oil spills and the surface of the sea made it possible to eliminate several ambiguities in the process.

The results of identification obtained with the two networks are compared; CMOD4 and CMOD5 processes including the speed of wind provide more successful results with 89% and 99% of success rate against 83% for the first network. This work allowed us to appreciate the contribution of the evaluation and the interpretation of the atmospheric phenomena in the identification of the oil spills. We propose an application of oil spill detection service, through reception and analysis of the near real time satellite data, for early warning alerts the coast guard.

Other parameters related to the atmosphere such as the wind direction can be added at the entries of the network of neurons for improving the performance of the identification, for that an automation of the estimate of the wind direction must be carried out.

ACKNOWLEDGEMENTS

The authors wish to thank the European Space Agency (ESA) and the European Research Institute (ESRIN) for the providing of a complete set of satellite radar data SAR ERS 1 and 2 and the working structures of the ESA/ESRIN.

REFERENCES

- Bern T.I., Wahl T., Anderssen T. & Olsen R., 1993. Oil spill detection using satellite based SAR : experience from a field experiment. *Photogrammetric Engineering and Remote Sensing*, Vol. 59, N°3, March 1993, pp 423-428.
- Bouchaib S., Smara Y., Salvatori L., Del Frate F. & Lichtenegger J., 2004. Oil spill detection and identification using radar SAR data in the Mediterranean sea. *World Conference on Energy For Sustainable Development, Technology Advances & Environmental Issues*, 6-9 December 2004, Cairo, Egypt.
- Brekke C., Solberg Anne H.S., 2005. Oil spill detection by satellite remote sensing. *Remote Sensing of Environment* 95 1-13 science direct ELSEVIER.
- Del Frate F., Petrocchi A., Lichtenegger J. and Calabresi G., 2000 , Neural networks for oil spill detection using ERS-SAR data. *IEEE Transactions of Geoscience and Remote Sensing*, vol. 38, n. 5, pp. 2282-2287.
- Espedal H. A. and Wahl T., 1999. Satellite SAR oil spill detection using wind history information, *Int. J. Remote Sensing*, vol. 20, no. 1, 49-65.
- Fontanel, N.A., 1973, La télédétection des pollutions, *Revue « Les cahiers français »*, N°163, notice 2, 1973.
- Hamre T., Espedal H., Samuel P. & Sandven S., 1996. *Operator's Manual for Slick Analysis*, NERSC Special Report, no.37.
- Hersbach H., Stofellen A. and S.de Haan , 2005. The improved C-band geophysical model function CMOD5 *Proc.of the 2004 Envisat & ERS Symposium*, 6-10 September 2004, Salzburg,Austria.
- Konstantinos N. Topouzelis, 2008. *Oil Spill Detection by SAR Images: Dark Formation Detection,Feature Extraction and Classification Algorithms*, sensors, ISSN 1424-8220,18
- Lecomte, 1993, *CMOD4 Model description* ,ESRIN DPE/OM, 8p.
- Mastin G. A., Harlow C.A., Huh O.K. And Hsu S. A., 1985. *Methods of Obtaining Offshore Wind Direction and Sea-State Data.From X-Band Aircraft SAR Imagery of Coastal Waters*. *IEEE of Oceanic Engineering*, vol. OE-10, no. 2.
- Stoffelen A &D Anderson, 1997, *Scatterometer data interpretation: Estimation and validation of the transfer function CMOD4*, *JGR* 102, 5767-5780.

BIOGRAPHICAL NOTES

Horiya KHENOUCHE received the Master degree in Telecommunications Systems from the 08 May 1945 university, Guelma, Algeria, in 2010. Her main interest was focused on identification of oil spills on sea surfaces from SAR radar remote sensing. She is actually following doctoral studies in Telecommunications and Information Processing, related to the Image Processing and Radiation Laboratory of the Faculty of Electronic and Computer Science of the Houari Boumediene University of Sciences and Technology of Algiers. Her interests concern remote sensing and image processing applied to SAR images.

Youcef SMARA is professor and director of research in the Image Processing and Radiance Laboratory of the Faculty of Electronic and Computer Science of the Houari Boumediene University of Sciences and Technology of Algiers. He is a director of the laboratory. He works since more of twenty years in the domain of image processing, remote sensing and GIS. He is author of more of hundred and fifty publications, international and regional communications.

CONTACTS

Horiya KHENOUCHE

E-mail: hkug19@hotmail.com

Professor Youcef SMARA

Image Processing and Radiation Laboratory,
Faculty of Electronics and Computer Science,
Houari Boumediene University of Sciences and Technology ((U.S.T.H.B)
BP 32 El-Alia Bab-Ezzouar 16111
Algiers,
ALGERIA
Fax: 213 21 24 71 87
Email : ysmara@usthb.dz ; yousmara@yahoo.com